

Dykens, Mass Spectrometry Facility, for their splendid assistance. Support by the University of Pennsylvania Research Fund and by the National Institutes of Health (Grant GM 38079) is gratefully acknowledged.

Supplementary Material Available: Tables of refined atomic positional and thermal parameters for the two X-ray structures reported (6 pages). Ordering information is given on any current masthead page.

11 K Charge Density Study of 2,5-Diaza-1,6-dioxa-6a-thiapentalene Containing a Short Nonbonded S...O Contact

B. Fabius,[†] C. Cohen-Addad,^{*,†} F. K. Larsen,[†] M. S. Lehmann,[§] and P. Becker^{||}

Contribution from the Department of Chemistry, Aarhus University, DK-8000 Aarhus C, Denmark, Laboratoire Spectrométrie Physique, University of Grenoble, BP 87, 38402 Saint Martin d'Hères, France, Institut Laue-Langevin, BP 156, 38042 Grenoble, France, and Laboratoire Cristallographie, CNRS, BP 166, 38042 Grenoble, France.

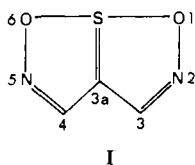
Received July 12, 1988

Abstract: In the compound 2,5-diaza-1,6-dioxa-6a-thiapentalene, the S...O distance is 1.83 Å, which is intermediate between a covalent bond length and the sum of the atomic van der Waals radii. The charge density distribution in the molecule was not clearly understood from previous 122 K X-ray and neutron measurements. In the present study, results obtained with 11 K X-ray diffraction measurements and aspherical atom refinement using the program MOLLY are presented. The static deformation model maps are in good agreement with the theoretical maps obtained from a previous local density functional calculation. The mechanism proposed to interpret the X-S...O interaction depends on the electronegativity of X and involves a σ -type coupling between oxygen and sulfur p orbitals. Furthermore, the molecule is stabilized through sulfur d orbitals. The experimental charge distribution obtained at 11 K supports this theory. The 11 K study is more conclusive than the previous 122 K study, which used a spherical treatment of the electron density distribution. It leads to the rejection of the controversial deduction that oxygen is in a spherical state with little hybridization. A reinvestigation of the previous 122 K X-ray data using the MOLLY program is qualitatively consistent with these results, although strongly influenced by the thermal effects.

Many compounds containing the X-S...O configuration (X = O, C) exhibit very short X...O contacts.^{1a,b} The S...O distance varies between 1.83 and 2.96 Å. This is longer than the covalent S-O bond length of 1.56-1.65 Å^{1b} yet much shorter than the sum of the van der Waals radii, which is 3.3 Å.² In previous studies by X-ray and neutron diffraction on compounds with S...O contacts of 2.24 and 2.68 Å,^{3a,b,4} the X-N deformation electron density maps showed only weak features in the sulfur-oxygen region. This finding was not concordant with theoretical analysis,^{3b,5} which showed that in these compounds the X-S...O attraction is mainly due to interactions between p nonbonded orbitals of the oxygen atom and p and d orbitals of sulfur.

In thiapentalene derivatives where X = O the molecules are planar and show a symmetrical conjugated structure;^{1b} the system O...S...O is symmetric, and the S...O distance is about 1.85 Å.

In order to gain insight in the molecular stabilization in these compounds, we have undertaken an investigation of the charge density in 2,5-diaza-1,6-dioxa-6a-thiapentalene (I). In a previous



work,⁴ we obtained experimental deformation electron density from a refinement of combined 122 K X-ray and neutron diffraction data using a radial deformation model. Electron density deformation maps showed a very diffuse O...S...O region, and little

positive density was observed in the lone-pair region of the oxygen atoms. This was in contradiction to the theoretical maps obtained by a local density function calculation.⁵

A multipole refinement using also combined 122 K X-ray and neutron diffraction data led to controversial conclusions about the density in the region around sulfur and oxygen.⁵

In order to clarify this point, we undertook an X-ray diffraction study at 11 K on I.

Experimental Section

Crystals of 2,5-diaza-1,6-dioxa-6a-thiapentalene were grown from cyclohexane solution. The crystal used for data collection was bounded by nine well-developed faces and had a volume of 0.0091 mm³ with the longest dimension 0.3 mm. It was mounted in a thin-walled capillary to prevent sublimation.

Data were collected at 11 ± 1 K using Nb-filtered Mo K α radiation ($\lambda = 0.7107$ Å). The crystal was cooled in a two-stage closed-cycle helium cryostat, a modified DISPLEX CS201 (manufactured by Air Products and Chemicals, Inc., and now by Intermagnetics General Corp.) mounted on a HUBER diffractometer.⁶ Low-temperature unit cell dimensions were checked several times during the data collection period,

(1) (a) Pedersen, C. Th. *Sulfur Rep.* **1980**, 1. (b) Bernardi, F.; Cszimadia, I. G.; Mangini, A. *Studies in Organic Chemistry. Organic Sulfur Chemistry*; Elsevier: Amsterdam, The Netherlands, 1985; Vol. 19.

(2) Pauling, L. *The Nature of the Chemical Bond*; Cornell University Press: Ithaca, New York, 1960; p 260.

(3) (a) Cohen-Addad, C.; Savariault, J. M.; Lehmann, M. S. *Acta Crystallogr.* **1981**, B37, 1703-1706. (b) Cohen-Addad, C.; Lehmann, M. S.; Becker, P.; Parkanyi, L.; Kalman, A. *J. Chem. Soc., Perkins Trans.* **2** **1984**, 191-196.

(4) Cohen-Addad, C.; Lehmann, M. S.; Becker, P.; Davy, H. *Acta Crystallogr.* **1988**, B44, 522-527.

(5) Becker, P.; Cohen-Addad, C.; Delley, B.; Hirshfeld, F. L.; Lehmann, M. S. *Applied Quantum Chemistry*; Smith, V. H., Jr., et al., Eds.; Reidel: Dordrecht, The Netherlands, 1986; pp 361-373.

(6) Henriksen, K.; Larsen, F. K.; Rasmussen, S. E. *J. Appl. Crystallogr.* **1986**, 19, 390-394.

[†] Aarhus University.

[†] University of Grenoble.

[§] Institut Laue-Langevin.

^{||} CNRS.

Table I. 2,5-Diaza-1,6-dioxo-6a-thiapentalene: Crystallographic Data for the 11 K Study

$M_r = 130.12$
space gp $P2_1/c$
$Z = 4$
unit cell dimens at 11 ± 1 K
$a = 6.762$ (2), $b = 6.925$ (2), $c = 10.903$ (3) Å; $\beta = 112.17$ (2)°
$V = 470.7$ (5) Å ³
$D_x = 1.83$ Mg m ⁻³
$\mu(\text{Mo K}\alpha) = 5.59$ cm ⁻¹
data set: $\pm h, k, l$ for $2\theta \leq 125^\circ$ and further; $\pm h, -k, l$ for $2\theta \leq 50^\circ$
scan mode: $\omega/2\theta$
scan range: $\Delta 2\theta = (1.4 + 0.7 \tan \theta)^\circ$
step scanned: 50 steps, 2 s/step
$[(\sin \theta)/\lambda]_{\text{max}}: 1.25$ Å ⁻¹
no. of refln coll: 9508
no. of unique reflns: 7503
internal consistency $R_I(F^2) = \sum F^2 - \langle F^2 \rangle / \sum F^2: 0.0225$
$[(\sin \theta)/\lambda]_{\text{max}}$ used in the refinement: 0.95 Å ⁻¹
no. of unique reflns up to $[(\sin \theta)/\lambda] = 0.95$ Å ⁻¹ : 3224
no. of reflns used in the refinement: 2353
cutoff $I/\sigma(I): 3.0$
weighting scheme: $\sigma(I) = 2F_o\sigma(F) = [\sigma^2(I) + 0.004(F_o)^2]^{1/2}$; $w = 1/\sigma(F)^2$
no. of variables: 141
G (isotropic extinction coefficient): 0.08 (2)
refinement on F values for $R = \sum F_o - F_c / \sum F_o: 0.028$; for $wR = [\sum w(F_o - F_c)^2 / \sum wF_o^2]^{1/2} 0.043$
goodness of fit: 1.01

each time by least-squares refinement of the centered angle settings of at least 28 reflections.

Integrated intensities were evaluated by the minimal $\sigma(I)/I$ criteria.⁷ Three standard reflections (2,0,0; 0,3,4; 1,0,-10) were measured after every 50 reflections. The two less intense reflections 0,3,4 and 1,0,-10 had intensities that decayed linearly by 3.4% during the data collection period, while 2,0,0, which is by far the strongest reflection of the structure, actually increased by 4% in intensity. This latter effect was attributed to change in extinction effect, and subsequently intensities were scaled according to the two less intense standard reflections.

During data collection it was observed that occasionally the counting chain suffered from strong noise pulses. Reflection profiles were scrutinized individually for spikes, and reflections deemed to include noise were either remeasured or removed from the refinement. Data were corrected for absorption by Gaussian numerical integration.⁸ Transmission factors range from 0.877 to 0.936.

Table I summarizes crystal data and experimental data conditions. Reflections with $(\sin \theta)/\lambda < 1.25$ Å⁻¹ were collected, but high-order refinements and subsequent examinations of profiles revealed that for data at the highest angles the scan range appeared to have been chosen slightly narrow, which might give underestimated intensities. Inclusion of the high-order data in the refinement did not modify significantly the electron density parameters but increased their standard deviations and did bias the thermal parameters. Furthermore, the 122 K X-ray data set only extended to $(\sin \theta)/\lambda < 0.95$ Å⁻¹, so for better comparison it was decided to use a similar cutoff limit for the 11 K data.

Results

The atomic electron density is expressed in terms of pseudoatoms

$$\rho(r) = \sum_n \rho_n(r) \cdot P_n(r - r_n)$$

where $\rho_n(r)$ is the pseudoatom density for atom n located at position r_n and $P_n(r - r_n)$ is the probability distribution function for atomic position r_n . $\rho_n(r)$ is further expanded in terms of symmetry-adapted functions:⁹

$\rho_n(r) =$

$$P_c \rho_{\text{core}}(r) + P_v \kappa'^3 \rho_{\text{val}}(\kappa' r) + \sum_{l=0}^4 \kappa''^3 R_l(\kappa'' r) \sum_{m=-l}^l P_{lm} Y_{lm}(r/r)$$

$$R_l(r) = \frac{\xi^{n_l+3}}{(n_l + 2)!} r^{n_l} \exp(-\xi_l r)$$

(7) Lehmann, M. S.; Larsen, F. K. *Acta Crystallogr.* **1974**, *A30*, 580-584.

(8) Coppens, P.; Leiserowitz, L.; Rabinovich, D. *Acta Crystallogr.* **1965**, *18*, 1035-1038.

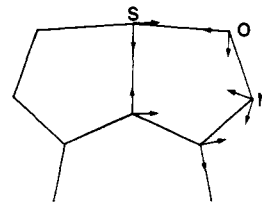


Figure 1. Choice of local cartesian axes for the multipole refinement. The third axis points out of the plane.

P_c , P_v , and P_{lm} are population coefficients, κ' and κ'' expansion-contraction coefficients, Y_{lm} is a real spherical harmonic function, and R_l is a STO radial function. The structure factor, the Fourier transform of the electron density distribution in the crystal, is expressed as

$$F(\mathbf{h}) = \sum_n \exp(2\pi i \mathbf{h} \cdot \mathbf{r}_n) T_n(\mathbf{h}) F_n(\mathbf{h})$$

$F_n(\mathbf{h}) =$

$$P_c f_{\text{core}}(\mathbf{h}) + P_v f_{\text{val}}(\mathbf{h}/\kappa') + \sum_{l=0}^4 \phi_l(\mathbf{h}/\kappa'') \sum_{m=-l}^l P_{lm} Y_{lm}(\mathbf{h}/\mathbf{h})$$

where T_n is the temperature factor, ϕ_l is the Fourier-Bessel transform of R_l .

A least-squares refinement minimizing the quantity $\sum w(|F_o| - k|F_c|)^2$ was performed with the program MOLLY⁹ on the 11 K X-ray data; w is defined in Table I and F_c refers to the $F(\mathbf{h})$ expression defined above. Extinction was treated isotropically in the type I Gaussian approximation¹⁰ and was found to be less than 1% on intensities for most reflections, except one reflection (2,0,0), which was affected by a factor of 23%; for another 7 reflections, the correction was between 2 and 6%. For non-hydrogen atoms, coordinates, anisotropic thermal parameters, and a multipole expansion of the valence shell up to hexadecapoles were refined.

Hartree-Fock functions were used for the monopoles. Scattering factor tables were taken from International Tables (Vol. IV, 1974) for non-hydrogen atoms and from ref 13 for hydrogen atoms. The parameters n_l and ξ_l of the radial part of the multipolar expansion were taken from ref 9. P_c was not varied since core electrons are not believed to play any important role. κ'' was maintained fixed to 1.0, since it was highly correlated with κ' . κ' values were kept fixed at 1.4 for hydrogen monopoles according to ref 12 and were refined for non-hydrogen atoms.

In order to reduce the number of variables, symmetry constrains were imposed on the molecule, based on the approximate C_{2v} symmetry observed in spherical atom refinements of the 11 K data and of data collected at higher temperatures:^{4,11} although non-crystallographically equivalent, the two halves of the molecule have bond lengths that are not significantly different and the molecule is nearly planar. Introduction of the C_{2v} constraint reduces the number of multipole parameters to 9 for S and C(3a) and 15 for the other non-hydrogen atoms. The local atomic coordinate systems are indicated in Figure 1. The refinement depended slightly on the orientation of the local axes, which reveals the incompleteness of an expansion limited to $l = 4$. The final choice of orientation was based on chemical intuition related to the expected hybridization state for each atom. The total thermal displacement is the sum of the contributions from internal and external modes of motion. The spherical atom least-squares refinement based on the 11 K X-ray showed that the atomic mean-square amplitudes were reduced by a factor of 3 relative to those found in the 122 K study. This shows that the relative

(9) Hansen, N. K.; Coppens, P. *Acta Crystallogr.* **1978**, *A34*, 909-921.

(10) Becker, P.; Coppens, P. *Acta Crystallogr.* **1975**, *A31*, 417-425.

(11) Amundsen, F. A.; Hansen, N. K.; Hordvik, A. *Acta Chem. Scand.* **1982**, *A36*, 673-681.

(12) Coppens, P.; Guru Row, T. N.; Leung, P.; Stevens, E. D.; Becker, P.; Yang, Y. W. *Acta Crystallogr.* **1979**, *A35*, 63-72.

(13) Stewart, R. F.; Davidson, E. R.; Simpson, W. T. *J. Chem. Phys.* **1965**, *42*, 3175-3187.

Table II. 2,5-Diaza-1,6-dioxo-6a-thiapentalene: Atomic Coordinates and Thermal Parameters at 11 K

atoms	<i>x</i>	<i>y</i>	<i>z</i>	B_{eq}^a , Å ²
S	0.76625 (3)	0.09687 (3)	0.07344 (2)	0.36 (2)
O(1)	0.7754 (2)	-0.1307 (1)	-0.0108 (1)	0.53 (3)
O(6)	0.7425 (2)	0.3028 (1)	0.1731 (1)	0.50 (3)
N(2)	0.7622 (2)	-0.2884 (1)	0.0567 (1)	0.53 (3)
N(5)	0.7197 (2)	0.2521 (1)	0.2853 (1)	0.52 (3)
C(3)	0.7476 (2)	-0.2422 (1)	0.1701 (1)	0.47 (3)
C(3a)	0.7462 (1)	-0.0423 (1)	0.1946 (1)	0.40 (3)
C(4)	0.7240 (2)	0.0638 (1)	0.2995 (1)	0.49 (3)
H(3)	0.7362	-0.3555	0.2339	1.65
H(4)	0.7097	-0.0010	0.3859	1.65

$$^a B_{\text{eq}} = 8\pi^2(u_1u_2u_3)^{2/3}.$$

weight of internal versus external modes increases when the temperature is reduced.

We assume that the internal motion in the C-H bond does not change in going from 122 to 11 K. Therefore, the thermal parameters of the hydrogen atoms were estimated according to the formula

$$B_{11\text{K}}(\text{H}) = \frac{1}{3}(B_{122\text{K}}(\text{C})) + (B_{122\text{K}}(\text{H}) - B_{122\text{K}}(\text{C}))$$

where $B_{122\text{K}}(\text{C})$ is the isotropic B value equivalent to the anisotropic β tensor for carbon at 122 K.

In order to counteract in the deformation maps the effect of artificial shortening of terminal bonds determined by refinement of X-ray data only, the 11 K coordinates of hydrogen atoms were calculated from the 122 K neutron data refinement and kept fixed, as well as their thermal parameters.

The results of the refinement are reported in Table I. Atomic and thermal parameters are given in Table II, and bond lengths and valence angles are reported in Table III and compared to the values obtained at 122 K (Lists of h, k, l, F_o , and F_c of multipole coefficients and anisotropic thermal parameters are given as supplementary material for 11 K and 122 K data refinements.) The geometry of the molecule is identical at the two temperatures. The bond length of the central S-C(3a) is close to that of a S=C double bond. The molecule is nearly planar; the halves of the molecule form an angle of 2.5 (1)°.

The deviation from spherical electron density due to chemical bonding is shown as static deformation model maps in two sections through the molecule (Figure 2). On these maps, the spherical hydrogen atoms are not subtracted. They correspond to calculated structure factors with $(\sin \theta)/\lambda \leq 1.0 \text{ \AA}^{-1}$. The effect of series termination is negligible at this resolution. Dynamic deformation maps were also calculated. They were practically identical with the static ones. This reflects the very small effect of thermal motion at 11 K.

Discussion

Theoretical deformation model maps shown on Figure 3 were obtained from a local density functional calculation using a spherical Coulomb potential and polarized numerical basis set (hydrogen atoms not subtracted). This calculation was discussed in detail in ref 5. The basis set was not optimized at the molecular

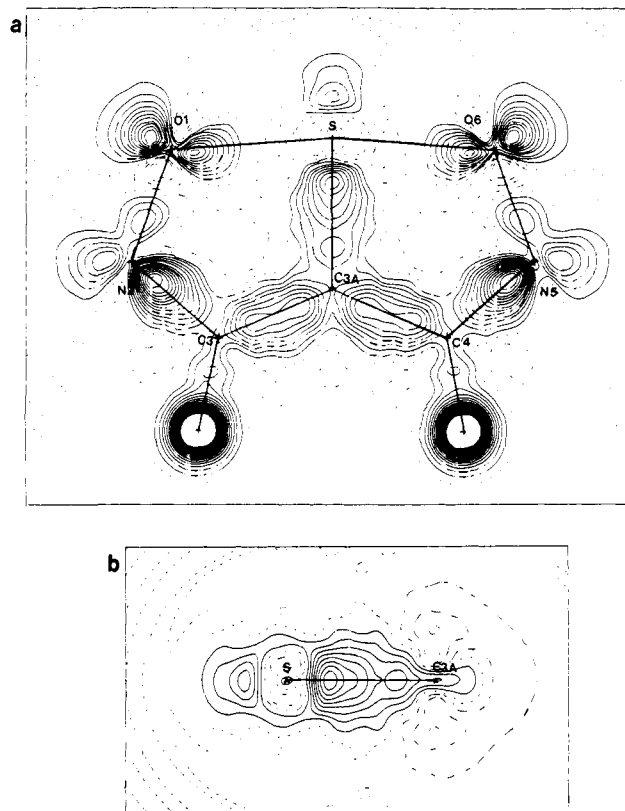


Figure 2. 2,5-Diaza-1,6-dioxo-6a-thiapentalene: static deformation model maps at 11 K. Contour intervals: 0.1 e Å⁻³. Spherical hydrogen atoms are not subtracted; (a) molecular plane; (b) plane perpendicular to the molecular plane and containing the S-C(3a) bond.

level, but only for atoms. Change in the basis had very little effect on the main features of the electron density.

We observe a good agreement between the experimental and theoretical maps. The shapes and magnitudes of the p overlap between bonded atoms for the C-C, C-N, and C-S bonds are in very good correspondence. The orientation of the positive lobes of the deformation density around oxygens is also concordant between theory and experiment. The anisotropy of the electron density around oxygen is much more pronounced in the theoretical than in the experimental maps, leading to some differences in the peak heights. The lone-pair peak of the nitrogens is much smaller in the experimental than in the theoretical maps. The positive peak beyond the sulfur agrees with the theoretical prediction although it is significantly larger in the experimental map. Obviously, the same observation can be made for the map in the plane perpendicular to the molecular plane and containing the S-C(3a) bond. The experimental net charges are given in Table IV. The dipole moment directed along the S-C bond corresponding to the map is 2 (1) D, which is consistent with measured value of 2.88 (2) D.¹⁴ This dipole moment was calculated from the monopole

Table III. 2,5-Diaza-1,6-dioxo-6a-thiapentalene. Comparison of Geometries for 11 and 122 K Structures

	bond lengths, Å		bond angles, deg	
	11 K	122 K	11 K	122 K
S-O(1)	1.837 (1)	1.834 (1)	O(6)-S-O(1)	171.64 (5)
S-O(6)	1.836 (1)	1.836 (1)	O(6)-S-C(3a)	85.94 (6)
S-C(3a)	1.682 (1)	1.6809 (8)	O(1)-S-C(3a)	85.93 (6)
O(1)-N(2)	1.338 (1)	1.338 (1)	S-O(1)-N(2)	113.80 (8)
O(6)-N(5)	1.337 (2)	1.336 (1)	S-O(6)-N(5)	113.80 (7)
N(2)-C(3)	1.317 (2)	1.316 (1)	O(1)-N(2)-C(3)	111.24 (9)
N(5)-C(4)	1.312 (2)	1.314 (1)	O(6)-N(5)-C(4)	111.30 (9)
C(3a)-C(3)	1.411 (2)	1.410 (1)	N(2)-C(3)-C(3a)	115.21 (10)
C(3a)-C(4)	1.413 (2)	1.410 (1)	N(5)-C(4)-C(3a)	115.13 (9)
C(3)-H(3)	1.07		S-C(3a)-C(3)	113.90 (8)
C(4)-H(4)	1.08		S-C(3a)-C(4)	113.72 (8)
			C(3)-C(3a)-C(4)	132.34 (10)
				171.56 (3)
				85.87 (3)
				85.98 (4)
				113.73 (4)
				113.84 (5)
				111.27 (5)
				111.20 (5)
				115.13 (5)
				115.22 (5)
				113.88 (5)
				113.85 (5)
				132.22 (5)

Table IV. 2,5-Diaza-1,6-dioxa-6a-thiapentalene: Experimental Atomic Net Charges at 11 K and Comparison with Charges at 122 K

atoms	charge		atoms	charge	
	11 K, e	122 K, e		11 K, e	122 K, e
S	+0.41 (13)	+0.64 (9)	C(3), C(4)	+0.02 (7)	-0.21 (6)
O(1), O(6)	-0.90 (6)	+0.32 (5)	C(3a)	+0.29 (10)	+0.34 (8)
N(2), N(5)	-0.18 (9)	-0.40 (8)			

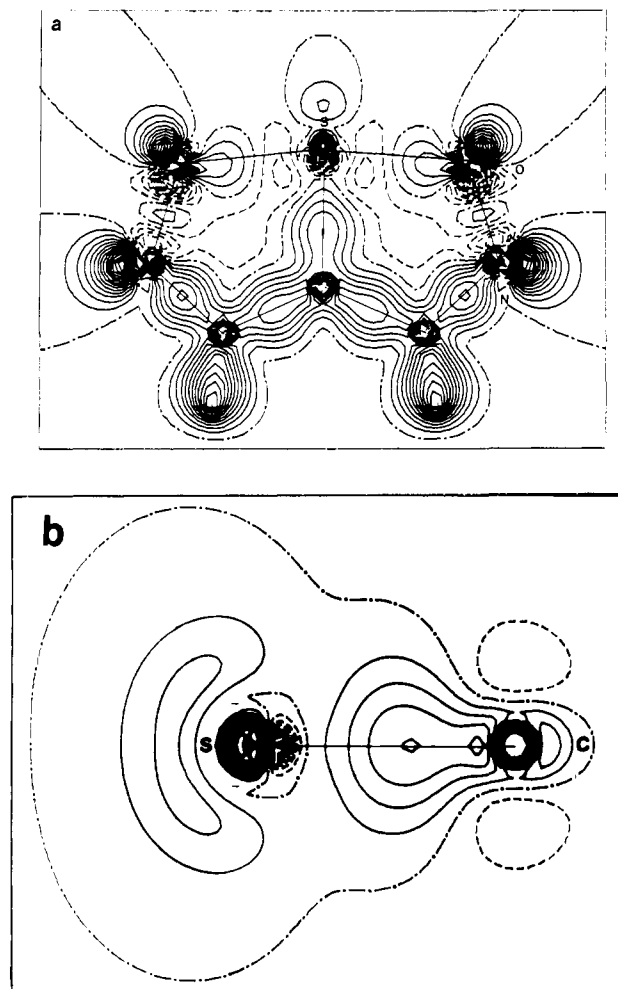
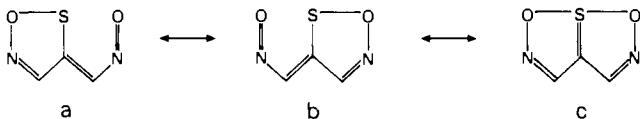


Figure 3. 2,5-Diaza-1,6-dioxa-6a-thiapentalene: theoretical deformation model maps. Contour intervals: $0.1 e \text{ \AA}^{-3}$. Spherical hydrogen atoms are not subtracted: (a) molecular plane; (b) plane perpendicular to molecular plane and containing the S-C(3a) bond.

and dipole coefficients of the refinement.

It was shown previously by extended Hückel calculations^{3b,5} that, in some compounds with relatively short distances (greater than 2.0 Å but less than the sum of the van der Waals radii),^{3b,5} the X-S...O interaction is governed by the electronegativity of X.

If X is less electronegative than O, the S...O distance is around 2.7 Å.^{1b} The interaction is weak and is essentially a d sulfur-p oxygen coupling, which overcomes the repulsion between sulfur and oxygen atoms. When X is oxygen, besides the stabilizing role of the d sulfur orbitals, a strong σ -type interaction between p_x orbitals of sulfur and oxygen along S...O leads to a shortening of the S...O distance, (x direction along S...O). The symmetrical configuration found for I suggests a resonance structure:



(14) Larsen, N. W.; Nygaard, L.; Pedersen, T.; Pedersen, C. Th.; Davy, H. *J. Mol. Struct.* **1984**, *118*, 89-95.

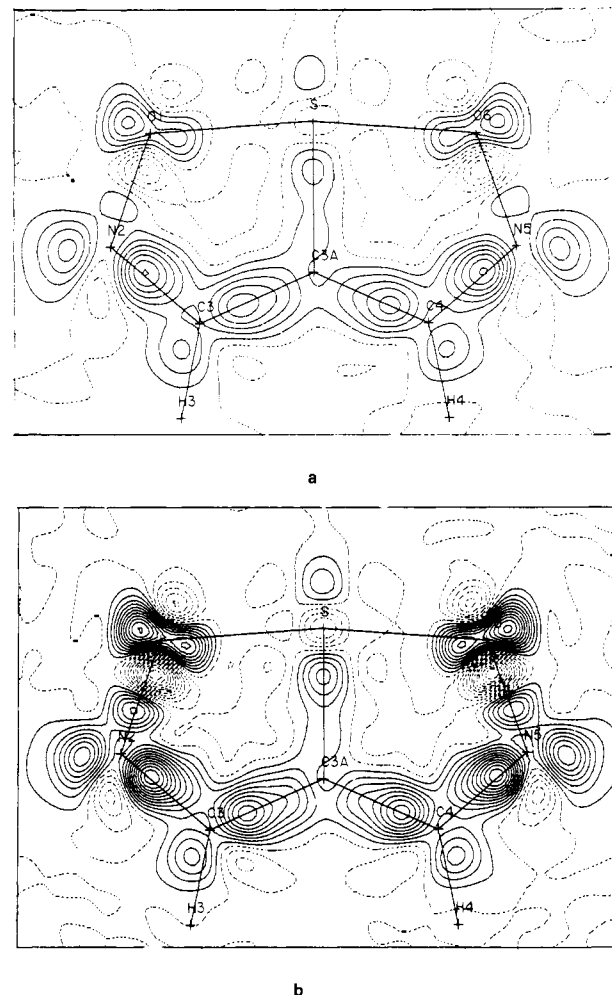


Figure 4. 2,5-Diaza-1,6-dioxa-6a-thiapentalene: dynamic (a) and static (b) deformation model map at 122 K in the molecular plane (spherical hydrogen atoms subtracted). Contour intervals $0.1 e \text{ \AA}^{-3}$.

A resonance between (a) and (b) would be consistent with the discussion presented above for an asymmetric case. However, they are inconsistent with the shortened S-C central bond observed in I. It indicates that the structure is best described by the symmetrical (c) form in which S is in a so-called hypervalent state, which is characterized by four electrons being accommodated in a three-center bond O-S-O. A strong $p(S)$ - $p(O)$ coupling occurs and the stability of the molecule is obtained by the inclusion of d orbitals on sulfur as in the asymmetrical structures. The hypervalent state of sulfur corresponds to one electron on a (sp_y) hybrid orbital toward C(3a), one σ lone pair in the orthogonal (s, p_y) hybrid, and one in p_x . One σ electron is promoted into the $d_{x^2-y^2}$ orbital and one π electron occupies the p_z orbital.

The π electronic structure of the molecule involves the contribution of one electron from sulfur, two electrons from each oxygen, and one electron from each nitrogen. As nitrogen is more electronegative than sulfur, the oxygen pair is more delocalized toward nitrogen than toward sulfur, and, thus, this increases the availability of sulfur orbitals for a π coupling with C(3a) giving a shortening of the S-C bond. This interpretation was supported by previous theoretical calculations^{5,15} and also by observations

(15) Faegri, K.; Støgaard, Å. *J. Mol. Struct.* **1977**, *41*, 271-279.

from several known symmetrical structures related to I.^{4,11,16,17} It is observed that if nitrogen is replaced by a carbon atom, the S-C central bond becomes longer.

This description is in agreement with observed as well as calculated electron densities. The form (c) would correspond to positive charge on sulfur and a negative charge on nitrogens, and this is indeed observed. The oxygen atoms are negatively charged. Moreover, the similar positive net charges on S and C(3a) favor a highly covalent interaction between these atoms, consistent with the observed S-C(3a) shortened distance. It is observed that the oxygen lobe facing sulfur is slightly lower than the lobe behind oxygen. This effect is related to the strong participation of the p_x orbital of oxygen to the three-center bonding O-S-O interaction. This dissymmetry in the oxygen deformation density is more clearly revealed on the theoretical map, and it was shown⁵ that going from a C-S...O to O-S...O and to O-S-O is accompanied by an increasing participation of the "x" lone-pair oxygen in the stabilizing interaction.

The result of the 11 K study led us to reexamine the 122 K X-ray data using the same aspherical type of refinement, as described above. The weighting scheme was the same as previously used in the radial model refinement.⁴ The hydrogen atom parameter was kept fixed at the values previously obtained.⁴ In the refinement ($R = 0.032$, $R_w = 0.034$, GOF = 1.51 for 2207 reflections) correlations of about 0.8 were observed between the scale factor and thermal parameters of sulfur and also between some multipole coefficients of oxygen. In the 11 K refinement no such high correlations were found. This emphasizes the role of thermal effects and may explain the great difference between the atomic charges obtained at 11 and 122 K (Table IV). The 122 K values are not consistent with the relative electronegativity of the different atoms. Nevertheless, the dynamic deformation density model map calculated in the molecular plane ($(\sin \theta/\lambda \leq 1.0 \text{ \AA}^{-1})$) and shown in Figure 4a presents the same general features as the 11 K study. However, the corresponding static deformation map (Figure 4b), although showing also the same features in the C-C, C-N, and C-S bonds, is strongly affected by the thermal effects, especially in the sulfur-oxygen region. This is not the case for the 11 K

study, where thermal effects are so small that the dynamic and static deformation model maps are practically identical.

Concluding Remarks

The use of the very low temperature X-ray diffraction data was decisive in the study of the charge density in 2,5-diaza-1,6-dioxo-6a-thiapentalene. The 11 K experimental deformation model maps, obtained after a multipole refinement with the MOLLY program⁹ are in good agreement with the maps obtained from a local density functional calculation and support the proposed mechanism for the S...O interaction.

A new investigation of the 122 K X-ray data using also the MOLLY program was in better qualitative agreement with these results than the previous studies, which used combined X-ray and neutron measurements,^{4,5} but it did reveal strong effects on the thermal vibrations. This could suggest that, at 122 K, the use of combined X-ray and neutron data may have biased the results because of differences in the X-ray and neutron thermal parameters.

These results emphasize the role of the thermal motions and the need of using very low temperature data for such an analysis.

A 120 K charge density study of a thiathiophene derivative (S...S...S interaction) was recently published¹⁸ in which the deformation maps, based on X-X spherical refinements, are very comparable to our results in the C-C and S-C regions. The S...S...S region, however, shows much less accumulation of positive density.

Acknowledgment. We are indebted to Prof. F. L. Hirshfeld for his interest in this study, to Prof. Y. Mollier for his collaboration, and to Dr. H. Davy for supplying the compound. B.F. was supported by a scholarship from the Carlsberg Foundation.

Registry No. 2,5-Diaza-1,6-dioxo-6a-thiapentalene, 57167-49-4.

Supplementary Material Available: Tables of multipole coefficients and anisotropic thermal parameters for the 11 K and 122 K data refinements (4 pages); listings of observed and calculated structure factors (29 pages). Ordering information is given on any current masthead page.

(16) Dalseng, M.; Hansen, K. L.; Hordvik, A. *Acta Chem. Scand.* **1981**, *A35*, 645-651.

(17) Llaguno, E. C.; Paul, I. C. *Tetrahedron Lett.* **1973**, *17*, 1565-1568.

(18) Wang, Y.; Chen, M. J.; Wu, C. H. *Acta Crystallogr.* **1988** *B44*, 179-182.